Article

Activity of Rhodium-Catalyzed Hydroformylation: Added Insight and Predictions from Theory

Manuel Sparta, Knut J. Brve, and Vidar R. Jensen

J. Am. Chem. Soc., **2007**, 129 (27), 8487-8499• DOI: 10.1021/ja070395n • Publication Date (Web): 08 June 2007

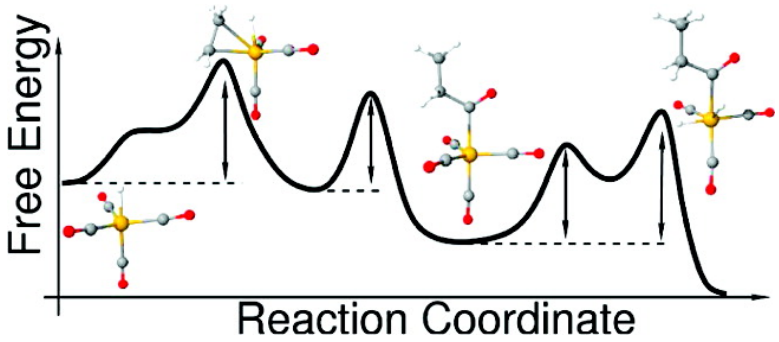

J|A|C|S
ARTICLES
Published on Web 06/08/2007

Activity of Rhodium-Catalyzed Hydroformylation: Added Insight and Predictions from Theory

Manuel Sparta, Knut J. Børve, and Vidar R. Jensen*

Contribution from the Department of Chemistry, University of Bergen, Allégaten 41, N-5007 Bergen, Norway

Received January 18, 2007; E-mail: Vidar.Jensen@kj.uib.no

Abstract: We have performed a density functional theory investigation of hydroformylation of ethylene for monosubstituted rhodium−carbonyl catalysts, $HRh(CO)_3L$, where the modifying ligand, L, is a phosphite ($L = P(OMe)_3$, $P(OPh)_3$, or $P(OCH_2CF_3)_3$), a phosphine ($L = PMe_3$, PEt_3, P^iPr_3, or PPh_3), or a N-heterocyclic carbene (NHC) based on the tetrahydropyrimidine, imidazol, or tetrazol ring, respectively. The study follows the Heck and Breslow mechanism. Excellent correspondence between our calculations and existing experimental information is found, and the present results constitute the first example of a realistic quantum chemical description of the catalytic cycle of hydroformylation using ligand-modified rhodium carbonyl catalysts. This description explains the mechanistic and kinetic basis of the contemporary understanding of this class of reaction and offers unprecedented insight into the electronic and steric factors governing catalytic activity. The insight has been turned into structure−activity relationships and used as guidelines when also subjecting to calculation phosphite and NHC complexes that have yet to be reported experimentally. The latter calculations illustrate that it is possible to increase the electron-withdrawing capacity of both phosphite and NHC ligands compared to contemporary ligands through directed substitution. Rhodium complexes of such very electron-withdrawing ligands are predicted to be more active than contemporary catalysts for hydroformylation.

1. Introduction

Hydroformylation, the conversion of an olefin, carbon monoxide, and molecular hydrogen into the corresponding aldehyde, is one of the most important industrial processes catalyzed by transition metal complexes in the homogeneous phase, with an annual production of aldehydes approaching 10 million tons.[1] Most of these aldehydes are subsequently hydrogenated to alcohols that are used as solvents (short-chain alcohols) or to make other chemical products such as detergents, plasticizers, lubricants, and pharmaceuticals.

The first hydroformylation catalysts were developed already in the late 1930s and were based on cobalt(I) carbonyl complexes.[2,3] Later, rhodium(I) carbonyl complexes proved to be even more active hydroformylation catalysts and also considerably more tolerant toward functional groups.[4] Unfortunately, the carbonyl complexes tended to give high ratios between branched and linear aldehyde products, and the introduction of phosphine-modified rhodium(I) complexes, in particular complexes containing arylphosphine ligands, drastically improved the ratio between branched and linear products.[5−8] Today, the bulk of hydroformylation processes are mediated by rhodium(I) triarylphosphine catalysts, resulting in high regioselectivities (i.e., toward linear aldehydes), a high tolerance toward various functional groups, and minimal problems with side reactions such as hydrogenation.[9,10]

In the early 1960s, Heck and Breslow proposed a reaction mechanism for hydroformylation catalyzed by cobalt carbonyl complexes.[11,12] This mechanism is analogous to Wilkinson's dissociative mechanism[6−8] and has later been accepted as the reaction route that most cobalt- and rhodium-catalyzed hydroformylation processes follow. Scheme 1 illustrates this mechanism adapted for the monosubstituted rhodium carbonyl catalysts, $HRh(CO)_3L$. It consists of the following steps: ligand dissociation to create a 16-electron species (**1** → **2**), olefin coordination (**2** → **3**), olefin insertion into the metal−H bond (**3** → **4** (via **TS1**)), CO coordination (**4** → **5**), CO insertion (**5** → **6** (via **TS2**)), H_2 oxidative addition (**6** → **8** (via **TS3**)), and, finally, reductive elimination of the aldehyde product (**8** → **2** (via **TS4**)).

The prevailing view in reviews[13,14] and textbooks[15−17] has been that oxidative addition of dihydrogen, **6** → **8**, is rate

(1) Bizzari, S.; Blagoev, M.; Kishi, A. Oxo Chemicals. In *Chemical Economics Handbook*; SRI Consulting: Menlo Park, CA, 2006.
(2) Roelen, O. Chemische Verwertungsgesellschaft Oberhausen m.b.H., German Patent DE 849,548 1938/1952; U.S. Patent 2,317066, 1943.
(3) Roelen, O. *Chem. Abstr.* **1944**, *38*, 550.
(4) Pruchnik, F. P. *Organometallic Chemistry of the Transition Elements*; Plenum Press: New York, 1990.
(5) Young, J. F.; Osborn, J. A.; Jardine, F. A.; Wilkinson, G. *J. Chem. Soc., Chem. Comm.* **1965**, 131.
(6) Evans, D.; Osborn, J. A.; Wilkinson, G. *J. Chem. Soc. A* **1968**, 3133.
(7) Evans, D.; Yagupsky, G.; Wilkinson, G. *J. Chem. Soc. A* **1968**, 2660.
(8) Brown, C. K.; Wilkinson, G. *J. Chem. Soc. A* **1970**, 2753.
(9) Parshall, G.; Ittel, S. *Homogeneus Catalysis*, 2nd ed.; Wiley: New York, 1992.
(10) Arnoldy, P. In *Rhodium Catalyzed Hydroformylation*; van Leeuwen, P. W. N. M., Clever, C., Eds.; Kluwer Academic Publishers: Dordrecht, The Netherlands, 2000.
(11) Breslow, D. S.; Heck, R. F. *Chem. Ind. London* **1960**, 467.
(12) Heck, R. F.; Breslow, D. S. *J. Am. Chem. Soc.* **1961**, *83*, 4023.
(13) Torrent, M.; Sola, M.; Frenking, G. *Chem. Rev.* **2000**, *100*, 439.

Scheme 1. Heck and Breslow Mechanism[11,12] for Hydroformylation of Ethylene as Adapted for Monosubstituted Rhodium Carbonyl Complexes, $HRh(CO)_3L$

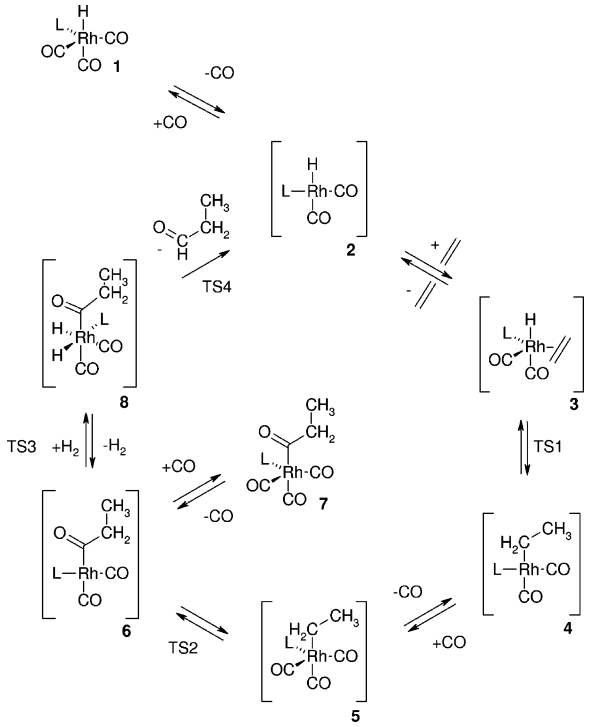

determining. However, in recent years substantial evidence has shown that, under normal industrial conditions, this is not the case, at least not for most ligand-modified catalysts.[18−23] The confusion as to the overall rate-determining step of the hydroformylation reaction to a large extent originates from the fact that hydroformylation reactions are extremely sensitive to the exact makeup of the catalyst, the experimental conditions, and the alkene substrate.[19,24] In fact, detailed mechanistic studies have shown that the rate-determining step may depend strongly on the exact conditions used.[20,24] In other words, several of the reaction steps must be associated with barriers of comparable heights.[19] The competition between these barriers makes it difficult to analyze and understand the effect on reaction rate or selectivity resulting from even small variations in catalyst structure or reaction conditions in experiments, as these changes may cause opposite responses in the individual elementary steps. In addition, experimental investigations of structure−activity and structure−selectivity relationships are obscured by the presence of a mixture of 18-electron "resting" complexes $HRh(CO)_mL_n$ ($m + n = 4$).[19,25] Molecular-level computational methods may ameliorate the situation by addressing the activity and selectivity for each potentially active structure. Force-field-based methods have already contributed structure−activity and structure−selectivity relationships in the form of the natural-bite-angle concept[26] which has proved to be a practical and highly useful tool in the development of active and selective catalysts based on diphosphine and diphosphite ligands. The contributions from the individual reaction steps may, in principle, be resolved using quantum chemical methods, which thus have a great potential for contributing valuable mechanistic information as well as playing a direct role in ligand optimization and catalyst development.

To date, quantum chemical studies of cobalt- and rhodium-catalyzed hydroformylation have followed the Heck and Breslow mechanism[11,12] and have confirmed that it constitutes a viable reaction route; see the reviews and seminal contributions[13,27−28] and references therein. The theoretical studies of rhodium-based catalysts have either explored essentially the entire Heck−Breslow catalytic cycle[30−36] or focused in detail on selected parts thereof.[37−42] The studies of the catalytic cycle have added much insight and detail to the Heck−Breslow mechanism, but it is not easy to argue that these studies have provided calculated potential energy surfaces (PESs) that are in accord with the currently available experimental information about the kinetics and mechanism for the different classes of rhodium catalysts for hydroformylation. For example, in a series of studies of hydroformylation of ethylene using the complexes $HRh(CO)_3PH_3$ or $HRh(CO)_2(PH_3)_2$ as models for phosphine-substituted rhodium catalysts,[30−33] the CO insertion step was calculated to have the highest barrier. However, it was concluded[13,30−33] that, if solvent effects were included, the oxidative addition of H_2 probably would represent the rate-determining step. Even in the most recent quantum chemical studies of olefin hydroformylation using phosphine-modified rhodium carbonyl catalysts, H_2 addition was found to be rate limiting.[35,36] In contrast, and as pointed out by Gleich and Hutter,[34] the current consensus is that alkene coordination or insertion is rate determining in hydroformylation using phosphine-modified catalysts.[18−23] One would, accordingly, expect the corresponding parts of the calculated PESs to be associated with high free energies of activation. However, Gleich and Hutter[34] noted that an "unequivocal statement about the step

(14) Cornils, B. In *New Syntheses with Carbon Monoxide*; Falbe, J., Ed.; Springer-Verlag: Berlin, 1980.
(15) Tolman, C. A.; Faller, J. W. In *Homogeneous Catalysis with Metal Phosphine Complexes*; Pignolet, L. H., Ed.; Plenum Press: New York, 1983.
(16) Cotton, F.; Wilkinson, G.; Gaus, P. *Basic Inorganic Chemistry*, 2nd ed.; Wiley: New York, 1987.
(17) Cotton, F.; Wilkinson, G. *Advanced Inorganic Chemistry*, 5th ed.; Wiley: New York, 1988.
(18) Kiss, G.; Mozeleski, E. J.; Nadler, K. C.; VanDriessche, E.; DeRoover, C. *J. Mol. Catal. A: Chem.* **1999**, *138*, 155.
(19) van Leeuwen, P. W. N. M.; Casey, C. P.; Whiteker, G. T. In *Rhodium Catalyzed Hydroformylation*; van Leeuwen, P. W. N. M., Clever, C., Eds.; Kluwer Academic Publishers: Dordrecht, The Netherlands, 2000.
(20) van der Slot, S. C.; Kamer, P. C. J.; van Leeuwen, P. W. N. M.; Iggo, J. A.; Heaton, B. T. *Organometallics* **2001**, *20*, 430.
(21) Nozaki, K.; Matsuo, T.; Shibahara, F.; Hiyama, T. *Organometallics* **2003**, *22*, 594.
(22) van Leeuwen, P. W. N. M. *Homogeneous Catalysis: Understanding the Art*; Kluwer Academic Publishers: Dordrecht, The Netherlands, 2004.
(23) Kuil, M.; Soltner, T.; van Leeuwen, P. W. N. M.; Reek, J. N. H. *J. Am. Chem. Soc.* **2006**, *128*, 11344.
(24) van Rooy, A.; de Bruijn, J. N. H.; Roobeek, K. F.; Kamer, P. C. J.; van Leeuwen, P. W. N. M. *J. Organomet. Chem.* **1995**, *507*, 67.
(25) Kamer, P. C. J.; Reek, J. N. H.; van Leeuwen, P. W. N. M. In *Rhodium Catalyzed Hydroformylation*; van Leeuwen, P. W. N. M., Clever, C., Eds.; Kluwer Academic Publishers: Dordrecht, The Netherlands, 2000.
(26) Casey, C. P.; Whiteker, G. T. *Isr. J. Chem.* **1990**, *30*, 299.
(27) Ujaque, G.; Maseras, F. *Struct. Bond* **2004**, *112*, 117.
(28) Folga, E.; Ziegler, T. *J. Am. Chem. Soc.* **1993**, *115*, 5169.
(29) Ziegler, T.; Versluis, L. *Adv. Chem. Ser.* **1992**, 75.
(30) Musaev, D. G.; Matsubara, T.; Mebel, A. M.; Koga, N.; Morokuma, K. *Pure Appl. Chem.* **1995**, *67*, 257.
(31) Musaev, D. G.; Morokuma, K. *Adv. Chem. Phys.* **1996**, *95*, 61.
(32) Matsubara, T.; Koga, N.; Ding, Y. B.; Musaev, D. G.; Morokuma, K. *Organometallics* **1997**, *16*, 1065.
(33) Decker, S. A.; Cundari, T. R. *Organometallics* **2001**, *20*, 2827.
(34) Gleich, D.; Hutter, J. *Chem.—Eur. J.* **2004**, *10*, 2435.
(35) Luo, X. L.; Tang, D. Y.; Li, M. *THEOCHEM* **2005**, *714*, 61.
(36) Luo, X. L.; Tang, D. Y.; Li, M. *Int. J. Quantum Chem.* **2005**, *105*, 108.
(37) Koga, N.; Jin, S. Q.; Morokuma, K. *J. Am. Chem. Soc.* **1988**, *110*, 3417.
(38) Schmid, R.; Herrmann, W. A.; Frenking, G. *Organometallics* **1997**, *16*, 701.
(39) Carbo, J. J.; Maseras, F.; Bo, C.; van Leeuwen, P. W. N. M. *J. Am. Chem. Soc.* **2001**, *123*, 7630.
(40) Decker, S. A.; Cundari, T. R. *J. Organomet. Chem.* **2001**, *635*, 132.
(41) Decker, S. A.; Cundari, T. R. *New J. Chem.* **2002**, *26*, 129.
(42) Luo, X. L.; Tang, D. Y.; Li, M. *THEOCHEM* **2005**, *730*, 177.

with the highest reaction barrier" could not be made based on their calculations. That the hydroformylation reaction represents a challenge for quantum chemistry is furthermore illustrated by the fact that no "clear picture about activity differences" among the catalysts emerged from their detailed comparison of $HRh(CO)_4$ and three phosphine-modified complexes, $HRh(CO)_2L_2$ ($L = PF_3$, PH_3 and PMe_3). Gleich and Hutter did, however, note that olefin binding becomes thermodynamically more favorable as the basicity of the ligand, L, decreases, and this result correlates with the observed higher catalytic activity of $HRh(CO)_4$ and catalysts modified by electron-withdrawing ligands.[23,43,44] One possible explanation for the discrepancies with respect to experimental observation is the model character[34] of the ligands used so far in most studies of hydroformylation. The real phosphines employed in research and industry have so far only been used in the classical mechanical part of QM/MM studies of the olefin insertion step,[39−41] whereas the quantum chemical description of the phosphine ligands has been limited to PH_3. This approach is well suited for the treatment of steric effects from the bulky phosphines, as in the studies of regioselectivity of propene hydroformylation,[39,40] but may fail if electronic effects from the phosphine ligands are important.[45]

Whereas the aforementioned mixtures of 18-electron complexes, $HRh(CO)_mL_n$ ($m + n = 4$),[19,25] present in solution during hydroformylation using bulky phosphite ligands, are known to consist exclusively of monosubstituted complexes, $HRh(CO)_3L$,[46] the disubstituted compounds, $HRh(CO)_2L_2$, dominate in the standard case of $L = PPh_3$.[6−8,15,47−49] According to the dissociative mechanism,[6−8,11,12] the 18-electron complexes have to dissociate a CO or a modifying ligand to bind the alkene substrate and initiate hydroformylation. Kinetic modeling based on a broad range of kinetic data for $L = PPh_3$, recorded under industrial conditions, strongly suggests that the dominating active 16-electron species are only monosubstituted, i.e., $HRh(CO)_2L$.[18] The main focus of the present study will thus be on the activity of such monosubstituted 16-electron complexes, generated by dissociation of a carbonyl from $HRh(CO)_3L$. The choice of catalyst precursor, $HRh(CO)_3L$ versus $HRh(CO)_2L_2$, is not critical since dissociation of CO or PPh_3 from an 18-electron precursor is a fast process compared to hydroformylation.[48,50,51] This will ensure a clean investigation of the ligand effects on catalytic activity, avoiding the obscuring influence of the equilibria in which the 16- and 18-electron rhodium complexes are involved. In addition, the effects of disubstitution on the critical reaction barriers have been investigated for selected modifying ligands.

Finally, we have used a range of realistic ligands with a large variation in electronic and steric properties. The modifying ligands include phosphites ($L = P(OMe)_3$, $P(OPh)_3$, and $P(OCH_2CF_3)_3$), phosphines ($L = PMe_3$, PEt_3, P^iPr_3, and PPh_3),

Chart 1. Carbene Ligands Included in the Present Investigation

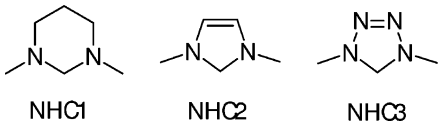

and N-heterocyclic carbenes (L = NHC1, NHC2, and NHC3; see Chart 1 for definition). In our calculations, we have followed the Heck and Breslow mechanism[11,12] for hydroformylation of ethylene using density functional theory (DFT).

2. Computational Details

A brief description of the computational approach is given in the following. Complete computational details are given in the Supporting Information.

2.1. Geometry Optimization. All geometry optimizations were performed with the OLYP density functional as implemented in Gaussian 03.[52] The OLYP functional consists of Handy's OPTX[53] modification of Becke's exchange functional and the correlation functional due to Lee, Yang, and Parr.[54]

Each stationary geometry was characterized by the eigenvalues of the analytically calculated Hessian matrix. The thermal corrections to enthalpies and Gibbs free energies at 80 °C were computed according to a procedure described in the Supporting Information.

Double-ζ Dunning−Huzinaga basis sets[55,56] were used for the light elements with contractions (4s)/[2s] for hydrogen and (9s5p)/[4s2p] for the first-row elements. For phosphorus, the Stuttgart relativistic 10-electron effective core potential (ECP) was used with an accompanying double-ζ valence basis set.[57] A single set of polarization d functions were added, resulting in a (4s,4p,1d)/[2s,2p,1d]-contracted basis set. The Stuttgart relativistic 28-electron ECP was used for Rh, with valence electrons described by an accompanying (8s,7p,6d)/[6s,5p,3d]-contracted basis set.[58]

2.2. Single-Point (SP) Energy Evaluations. The energy and all electronic properties were reevaluated at the optimized geometry, using Becke's three-parameter hybrid density functional (B3LYP)[59] as implemented in the Gaussian 03 suite of programs.[52]

Solvent effects for toluene were estimated by the polarizable continuum model (PCM)[60,61] using a reaction temperature of 80 °C. Atomic partial charges were calculated using natural population analysis (NPA).[62]

The basis sets used in the SP energy calculations were improved compared to those of the geometry optimizations. Hydrogen and elements of the first row were described using triple-ζ Dunning basis sets[63] extended with a single set of diffuse p functions (s for H) and a set of polarization d functions (p for H). For phosphorus, the (4s,4p,-1d) primitive set described above was extended by an even-tempered addition of a diffuse p function and contracted to give a valence triple-ζ set, [3s,4p,1d]. Finally, the details of all basis sets used are given in the Supporting Information.

(43) Unruh, J. D.; Christenson, J. R. *J. Mol. Catal.* **1982**, *14*, 19.
(44) van der Veen, L. A.; Boele, M. D. K.; Bregman, F. R.; Kamer, P. C. J.; van Leeuwen, P. W. N. M.; Goubitz, K.; Fraanje, J.; Schenk, H.; Bo, C. *J. Am. Chem. Soc.* **1998**, *120*, 11616.
(45) Bakowies, D.; Thiel, W. *J. Phys. Chem.* **1996**, *100*, 10580.
(46) Jongsma, T.; Challa, G.; Vanleeuwen, P. W. N. M. *J. Organomet. Chem.* **1991**, *421*, 121.
(47) Yagupsky, G.; Brown, C. K.; Wilkinson, G. *J. Chem. Soc. A* **1970**, 1392.
(48) Brown, J. M.; Canning, L. R.; Kent, A. G.; Sidebottom, P. J. *J. Chem. Soc., Chem. Commun.* **1982**, 721.
(49) Brown, J. M.; Kent, A. G. *J. Chem. Soc., Chem. Comm.* **1982**, 723.
(50) Kastrup, R. V.; Merola, J. S.; Oswald, A. A. *Adv. Chem. Ser.* **1982**, *196*, 43.
(51) Brown, J. M.; Kent, A. G. *J. Chem. Soc., Perkin Trans. 2* **1987**, 1597.
(52) Frisch, M. J. et al. *Gaussian 03*, revision C.02; Gaussian, Inc.: Wallingford, CT, 2004.
(53) Handy, N. C.; Cohen, A. J. *Mol. Phys.* **2001**, *99*, 403.
(54) Lee, C.; Yang, W.; Parr, R. G. *Phys. Rev. B* **1988**, *37*, 785.
(55) Dunning, Jr., T. H. *J. Chem. Phys.* **1970**, *53*, 2823.
(56) Dunning, T. H., Jr.; Hay, P. J. In *Modern theoretical chemistry*; Schaefer, H. F., III, Ed.; Plenum Press: New York, 1977.
(57) Bergner, A.; Dolg, M.; Kuchle, W.; Stoll, H.; Preuss, H. *Mol. Phys.* **1993**, *80*, 1431.
(58) Andrae, D.; Haeussermann, U.; Dolg, M.; Stoll, H.; Preuss, H. *Theor. Chem. Acc* **1990**, *77*, 123.
(59) Becke, A. D. *J. Chem. Phys.* **1993**, *98*, 5648.
(60) Tomasi, J.; Persico, M. *Chem. Rev.* **1994**, *94*, 2027.
(61) Cossi, M.; Scalmani, G.; Rega, N.; Barone, V. *J. Chem. Phys.* **2002**, *117*, 43.
(62) Reed, A. E.; Weinstock, R. B.; Weinhold, F. *J. Chem. Phys.* **1985**, *83*, 735.
(63) Dunning, T. H. *J. Chem. Phys.* **1971**, *55*, 716.

Table 1. Free Energies of the Stationary Points of Hydroformylation Catalyzed by Monosubstituted Rhodium Complexes, $HRh(CO)_3L$[a]

L	1	2	3	TS1	4	5	TS2	6	7	TS3	8	TS4
CO	0	31	37	84	8	−6	55	−29	−38	26	3	45
$P(OMe)_3$	0	23	48	97	29	15	66	−9	−35	33	5	49
$P(OPh)_3$	0	25	49	96	27	20	74	0	−30	42	15	55
$P(OCH_2CF_3)_3$	0	31	39	85	28	7	65	−12	−44	29	4	47
PMe_3	0	21	48	104	14	9	58	−29	−40	27	−6	37
PEt_3	0	18	56	110	28	27	69	−24	−33	33	−3	41
P^iPr_3	0	15	54	112	29	35	81	−7	−17	51	13	48
PPh_3	0	23	55	105	24	20	75	−8	−24	44	10	50
NHC1	0	−22	61	113	−36	6	64	−71	−37	30	4	42
NHC2	0	−3	59	107	−17	3	65	−59	−35	29	−7	37
NHC3	0	−2	52	102	−11	4	66	−53	−40	25	−10	35

[a] Energies are reported in kJ/mol and given relative to the sum of the energies of the reactants and $HRh(CO)_3L$. See Scheme 1 for labeling of the stationary points.

3. Results and Discussion

The present work follows the dissociative pathway as outlined in Scheme 1. The possibility of an associative pathway has been raised,[6] but solid experimental and theoretical evidence is now in favor of the dissociative mechanism; see the discussion in ref 34. Furthermore, only structures with the hydride ligand in an apical position will be considered, in accord with both experiment[64,65] and theory.[37,66,67] Moreover, the monosubstituted complexes studied all have the dative ligand L in the equatorial plane.[51,68,69] In the following, we will present results from a computational investigation of hydroformylation of ethylene catalyzed by the unmodified carbonyl complex, $HRh(CO)_4$, and a series of ligand-modified rhodium carbonyl complexes, $HRh(CO)_3L$. We have used phosphites (L = $P(OMe)_3$, $P(OPh)_3$, and $P(OCH_2CF_3)_3$), phosphines (L = PMe_3, PEt_3, P^iPr_3, and PPh_3), and N-heterocyclic carbenes (L = NHC1, NHC2, and NHC3; see Chart 1 for definition) as modifying ligands. The calculated free energies of hydroformylation are given relative to the sum of the energies of the reactants and $HRh(CO)_3L$ (or $HRh(CO)_4$ in the case of the unmodified catalyst) in Table 1; the corresponding enthalpies are given in the Supporting Information, as Table S1. The free energy curve for $HRh(CO)_4$ is shown in Figure 1, and those obtained for a selection of different catalysts are shown in Figure 2.

3.1. Unmodified Rhodium Carbonyl Complex. Dissociation of a CO ligand from the 18-electron monomeric precursor complex **1** leads to a square−planar 16-electron species, **2**; cf. Scheme 1. The unsaturated complex **2** coordinates ethylene to give **3** with the hydride in an apical position and ethylene bonded as a π complex in the equatorial plane; see the molecular structures in Figure 3. Both dissociation of CO and the coordination of ethylene are associated with an increase in free energy. Hence, the effective barrier in the initial part of the hydroformylation cycle consists of the sum of the energies required for the dissociation of CO, addition of ethylene to form the ethylene π complex (**3**), and for migratory insertion, **3** → **4** (via **TS1**); see Figure 1. This effective barrier will be referred to as $\Delta G^{\ddagger}_{TS1}$ in the following. TS1 has a close to trigonal bipyramidal geometry, with the hydride and one carbonyl in apical positions as in the case for **3** (Figure 3). Two of the positions in the equatorial plane are also still occupied by carbonyls, whereas the ethylenic carbon atom that is to form a new covalent bond to rhodium occupies the third position. Ethylene is oriented with the C−C bond parallel to the Rh−H bond. The structure is practically C_s-symmetric,[70] with the two OC−Rh−C(ethylene) angles in the equatorial plane both being close to 116°. The insertion of ethylene into the Rh−H bond leads to the four-coordinate, square planar alkyl complex **4**. In the presence of CO, **4** may coordinate a CO molecule to form **5**, and a migratory insertion of CO, **5** → **6** (via **TS2**), produces

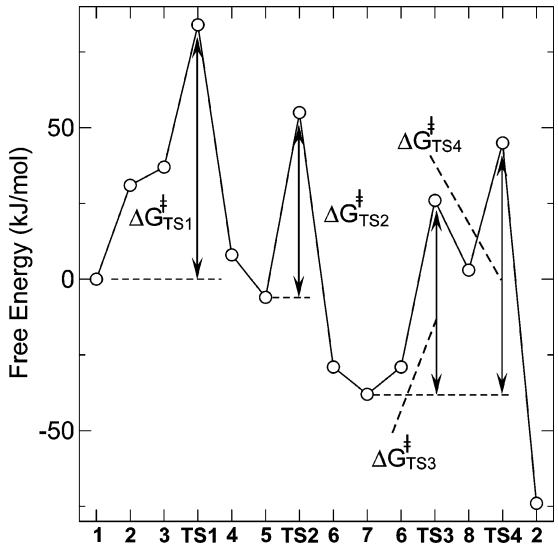

Figure 1. Free energy of hydroformylation of ethylene calculated for the $HRh(CO)_4$ catalyst precursor. The labels on the abscissa are consistent with Scheme 1. $\Delta G^{\ddagger}_{TS1}$, $\Delta G^{\ddagger}_{TS2}$, $\Delta G^{\ddagger}_{TS3}$, and $\Delta G^{\ddagger}_{TS4}$ represent the effective energy barrier of ethylene insertion, CO insertion, H_2 oxidative addition, and reductive elimination of the aldehyde product, respectively.

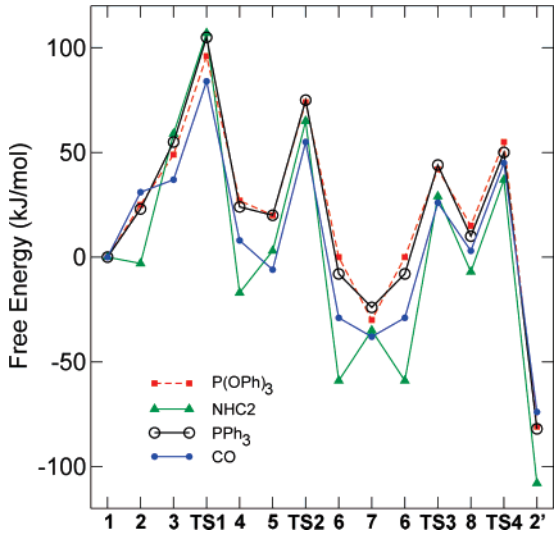

Figure 2. Free energy profile of hydroformylation of ethylene catalyzed by $HRh(CO)_3L$, L = PPh_3 (black circles), $P(OPh)_3$ (red squares), and NHC2 (green triangles). The profile for $HRh(CO)_4$ given for comparison (blue dots). The labels on the abscissa are consistent with Scheme 1.[75]

(64) Frenz, B. A.; Ibers, J. A. In *Transition Metal Hydrides*; Muetterties, E. L., Ed.; Modern theoretical chemistry; Marcel Dekker: New York, 1971.
(65) Vidal, J. L.; Walker, W. E.; Schoening, R. C. *Inorg. Chem.* **1981**, *20*, 238.
(66) Rossi, A. R.; Hoffmann, R. *Inorg. Chem.* **1975**, *14*, 365.
(67) Pidun, U.; Frenking, G. *Chem.—Eur. J.* **1998**, *4*, 522.
(68) Moser, W. R.; Papile, C. J.; Brannon, D. A.; Duwell, R. A.; Weininger, S. J. *J. Mol. Catal.* **1987**, *41*, 271.
(69) Kamer, P. C. J.; van Rooy, A.; Schoemaker, G. C.; van Leeuwen, P. W. N. M. *Coord. Chem. Rev.* **2004**, *248*, 2409.

(70) The slight deviation from a formally symmetric structure originates from the fact that the optimization was performed in C_1 symmetry; see the Computational Details.

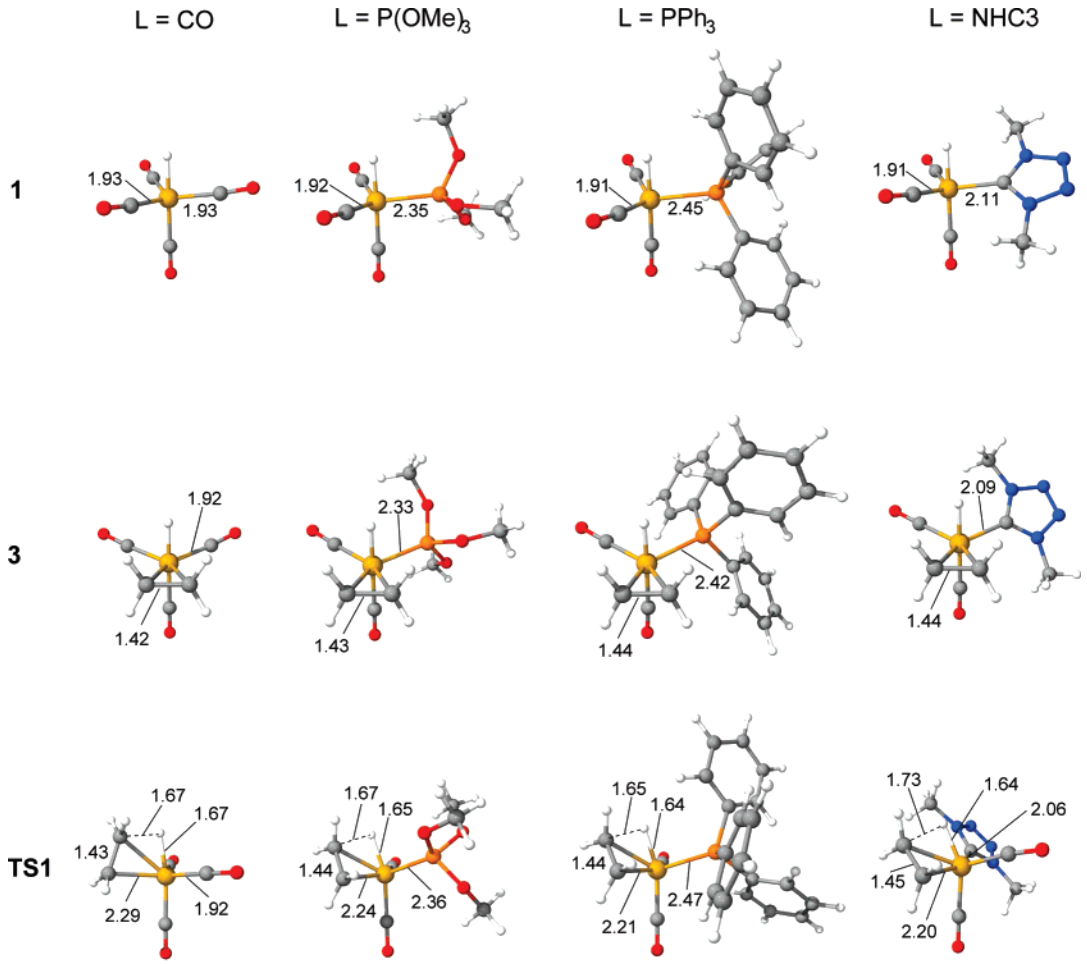

Figure 3. Molecular structures and selected distances (Å) for the complexes **1**, **3**, and **TS1** of the substrate coordination−insertion reaction for the catalysts $HRh(CO)_3L$, L = CO, $P(OMe)_3$, PPh_3, and NHC3.

the acyl complex, **6**. This elementary reaction is responsible for the second maximum on the PES with associated free-energy barrier $\Delta G^{\ddagger}_{TS2}$; see Figure 1.

According to our calculations, the saturated intermediate **7**, formed by complexation of CO to **6**, represents a dead end with respect to the catalytic reaction (Figure 4). In agreement with experimental observation[69,71−73] it is also the most stable intermediate. **7** thus represents a resting state and has to release CO in order to continue catalysis. The unsaturated acyl complex **6** may undergo oxidative addition of hydrogen, **5** → **6** (via **TS3**), to reach the rhodium(III) dihydride complex **8** from which reductive elimination of the aldehyde product, **8** → **2** (**TS4**), reforms the unsaturated active catalyst complex **2**. The dihydride complex, **8**, represents a relatively shallow minimum on the PES, in particular with respect to the back-reaction (dissociation of hydrogen), and the effective barrier to hydrogenolysis is best approximated as the energy difference between **TS4** and the resting state, **7**, indicated by $\Delta G^{\ddagger}_{TS4}$ in Figure 1.

Summarizing the above results, we can divide the hydroformylation cycle into three main sections: Alkene coordination and insertion, CO insertion, and hydrogenolysis. For the unmodified rhodium carbonyl catalyst, the associated effective free energy barriers $\Delta G^{\ddagger}_{TS1}$, $\Delta G^{\ddagger}_{TS2}$, and $\Delta G^{\ddagger}_{TS4}$ are given in Table 2. The calculated barriers to alkene insertion ($\Delta G^{\ddagger}_{TS1}$ = 84 kJ/mol) and hydrogenolysis ($\Delta G^{\ddagger}_{TS4}$ = 83 kJ/mol) are practically degenerate. The accuracy expected from our computational approach does not allow us to resolve the energy difference any further, in particular because these barriers stem from two different reactions. However, under normal reaction conditions the substrate concentration is an order of magnitude higher than the concentration of hydrogen, and this will shift the rate-controlling role toward the hydrogenolysis step. In addition, these barriers are calculated relative to the energies of carbonyl-saturated compounds, which for the hydrogenolysis reaction is the acyl rhodium tetracarbonyl resting state, (RC(O))$Rh(CO)_4$ (**7**). These results are in excellent agreement with the observation that the rate of hydroformylation with the unmodified rhodium−carbonyl catalyst is proportional to the concentration of hydrogen and inversely proportional to the concentration of CO.[19,73] CO insertion is associated with a significantly lower barrier ($\Delta G^{\ddagger}_{TS2}$ = 61 kJ/mol) than the other two steps. Our calculated relative energies for the individual elementary reaction steps are similar to those reported in other quantum chemical studies of rhodium−carbonyl-catalyzed hydroformylation of ethylene[34,74] and are, for example, within 10 kJ/mol from the corresponding DFT (BP86) energies obtained by Gleich and Hutter.[34] Gleich and Hutter obtained a higher

(71) Liu, G.; Volken, R.; Garland, M. *Organometallics* **1999**, *18*, 3429.
(72) Feng, J. H.; Garland, M. *Organometallics* **1999**, *18*, 417.
(73) Garland, M.; Pino, P. *Organometallics* **1991**, *10*, 1693.
(74) Alagona, G.; Ghio, C.; Lazzaroni, R.; Settambolo, R. *Organometallics* **2001**, *20*, 5394.

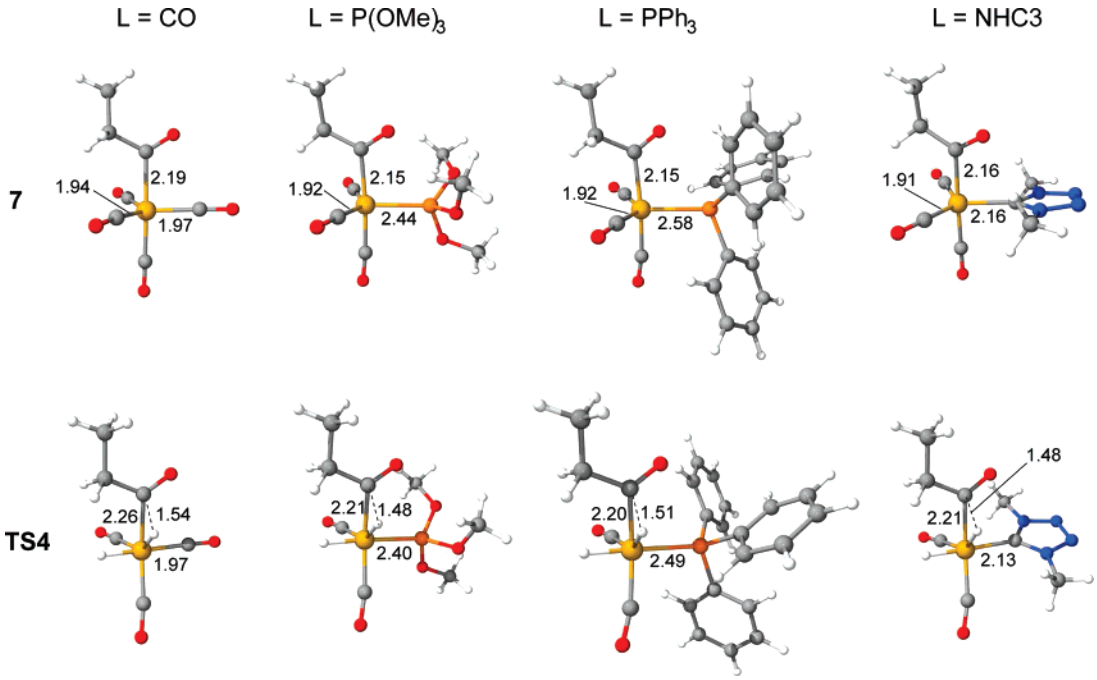

Figure 4. Molecular structures and selected distances (Å) for the complexes **7** and **TS4** of the hydrogenolysis reaction for the catalysts $HRh(CO)_3L$, L = CO, $P(OMe)_3$, PPh_3, and NHC3.

Table 2. Effective Free Energies and Enthalpies (in Parentheses) of Activation Calculated for the Catalysts $HRh(CO)_3L$[a]

L	$\Delta G^{\ddagger}_{TS1}$	$\Delta G^{\ddagger}_{TS2}$	$\Delta G^{\ddagger}_{TS4}$
CO	84 (79)	61 (60)	83 (85)
$P(OMe)_3$	97 (88)	51 (49)	84 (83)
$P(OPh)_3$	96 (93)	54 (55)	85 (84)
$P(OCH_2CF_3)_3$	85 (78)	58 (59)	91 (92)
PMe_3	104 (100)	49 (50)	77 (79)
PEt_3	110 (100)	42 (38)	77 (83)
P^iPr_3	112 (104)	52[b] (17)[b]	68[c] (61)[c]
PPh_3	105 (96)	55 (53)	74 (74)
NHC1	135[d] (97)[d]	100[b] (66)[b]	113[e] (86)[e]
NHC2	110[d] (70)[d]	82[b] (46)[b]	96[e] (61)[e]
NHC3	104[d] (60)[d]	77[b] (38)[b]	88[e] (54)[e]

[a] All energies are given in kJ/mol. [b] The barrier is calculated relative to **4**; see the relative free energies in Table 1. [c] **TS4** is lower in energy than **TS3** (Table 1), and therefore the barrier is computed for the step **7** → **TS3**. [d] The barrier is calculated relative to **2**; see the relative free energies in Table 1. [e] **6** is lower in energy than **7** (Table 1), and therefore the barrier is computed relative to **6**.

barrier to H_2 oxidative addition (**6** → **8** in Scheme 1) for the unmodified system than for the substituted complexes and concluded that this is commensurate with the first-order influence of hydrogen pressure on the rate of hydroformylation for the unmodified catalyst. We propose to adopt instead an effective barrier to hydrogenolysis ($\Delta G^{\ddagger}_{TS4}$, Figure 1), among other reasons because this definition implicitly includes the inhibiting effect of CO pressure due to the use of the resting state, **7** (not calculated in ref 34), as a reference state.

3.2. Monosubstituted Rhodium Carbonyl Complexes. 3.2.1. Phosphine and Phosphite Complexes. Substitution may change the free energy profile of hydroformylation significantly (Table 1) and, in particular, affect the barriers to coordination−insertion and hydrogenolysis. These kinetic parameters are listed in Table 2 for the full set of catalysts. Computed reaction energy profiles of hydroformylation for selected, representative modified catalysts are shown and compared with that of the unmodified catalyst in Figure 2. Whereas a bulky alkyl phosphine (L = P^iPr_3) gives a catalyst with a barrier to coordination−insertion almost 30 kJ/mol higher than that of the unmodified catalyst, the catalyst containing the strongly electron-withdrawing phosphite ligand $P(OCH_2CF_3)_3$ has a barrier for this reaction almost as low as the unmodified catalyst. The opposite trend can be seen for the hydrogenolysis reaction, for which the phosphine-modified catalysts actually have lower calculated barriers than the unmodified catalyst.

The PESs of hydroformylation for the phosphites are similar throughout the process and qualitatively resemble that presented above for $HRh(CO)_4$. Within the current set of ligands, the more electron-withdrawing ones, $P(OCH_2CF_3)_3$ and CO, are seen to destabilize the unsaturated complex **2**, i.e., to disfavor dissociation of CO. On the other hand, they afford an olefin complex (**3**) ca. 10 kJ/mol more stable than that of the other phosphite ligands (Table 1). Compared to the other phosphites, $P(OCH_2CF_3)_3$ and CO also facilitate ethylene insertion from the ethylene complex, albeit only by 1−3 kJ/mol. The overall result of the stabilization of the ethylene complex and the slightly facilitated insertion is a lowering of the effective barrier to coordination−insertion ($\Delta G^{\ddagger}_{TS}$) by more than 10 kJ/mol on going from L = $P(OMe)_3$ to $P(OCH_2CF_3)_3$; see Table 2. The positive effect that electron-withdrawing ligands can have on the early stages of the reaction is well-known, and, for example, Van Leeuwen and Roobeek noted remarkable reaction rates for complexes of strongly electron-withdrawing ligands such as the tris(2,2,2-trifluoroethyl) phosphite.[76] Kamer et al.[25] noted that both the high activities and selectivities of catalysts with strongly electron-withdrawing ligands could be explained by the "fast replacement of the carbonyl ligand by the alkene substrate".

(75) **2′** is the square planar product with the two carbonyl groups positioned trans to each other and the ligand L trans to the hydride ligand. **2′** may coordinate another CO and undergo Berry pseudorotations, with a low barrier,[38,37] to reach the precursor, **1**.

(76) Van, Leeuwen, P. W. N. M.; Roobeek, Shell, C. F.; Brit. Pat. 2 068 377, 1980; *Chem. Abstr.* **1984**, *101*, 191142.

Table 3. Tolman Parameters for the Presently Studied Phosphorus Ligands[a]

	PMe_3	PEt_3	P^iPr_3	PPh_3	$P(OMe)_3$	$P(OPh)_3$	$P(OCH_2CF_3)_3$
χ	7.8	5.4	3.0	12.9	23.1	29.1	42.9[b]
θ	118	132	160	145	107	128	115[c]

[a] Tolman angles are reported in degrees, and the electronic parameters, in cm^{-1}. [b] Reference 94. [c] No cone angle is available for $P(OCH_2CF_3)_3$. The cone angle of $P(OCH_2CCl_3)_3$ was used instead.[93]

The higher calculated stabilities of the olefin complexes (**3**) for the more electron-withdrawing ligands indeed confirm that a facilitated exchange reaction **1** → **3** is part of the explanation for the high activities.

As noted above, the olefin coordination and insertion steps are found to be clearly less facile for the complexes of alkyl and aryl phosphines. Even triphenyl phosphine, the most widely used modifying ligand in rhodium-catalyzed hydroformylation, gives an effective barrier ($\Delta G^{\ddagger}_{TS1}$) ca. 20 kJ/mol higher than that of the unmodified catalyst and ca. 10 kJ/mol higher than the corresponding phosphite, $P(OPh)_3$; see Table 2. In spite of the significant energy differences, the corresponding transition state geometries remain fairly similar among the different complexes; see Figure 3. As was the case for L = CO, the geometry of **TS1** may be characterized as a trigonal bipyramid (TBP), with the hydride and a carbonyl group representing the two axial ligands and the second CO, the ligand L, and the carbon atom that is to form a new covalent bond to rhodium being located in the equatorial plane. The transition state geometries of the modified catalysts, however, are more distorted from a TBP than the case for the unmodified catalyst. The carbon atom that is to form a new covalent bond to rhodium is now shifted toward the ligand L in the equatorial plane, with values below 100° for the L−Rh−C(ethylene) angle and in the range 145°−150° for OC−Rh−C(ethylene). A second set of transition state geometries, with wider angles for L−Rh−C(ethylene) than those for OC−Rh−C(ethylene), has been located at higher energies than those of the structures reported here. See also the discussion of the corresponding NHC complexes (*vide infra*).

All the phosphine complexes have their calculated rate-controlling barrier in the first part of the hydroformylation reaction (Table 2), whereas the most electron-withdrawing phosphite ($P(OCH_2CF_3)_3$) gives a catalyst with a higher effective barrier to hydrogenolysis ($\Delta G^{\ddagger}_{TS4}$ = 91 kJ/mol) than to coordination−insertion ($\Delta G^{\ddagger}_{TS1}$ = 85 kJ/mol). Whereas PMe_3 is predicted to provide catalytic activity similar to that of the popular aryl phosphine, PPh_3,[77] the higher alkyl phosphines are calculated to give less active catalysts than PPh_3, in accord with experimental comparison of, for example, the $HRh(CO)(PPh_3)_2$ and $HRh(CO)(PEt_3)_2$ catalysts.[6]

Summarizing, the calculated order that the different ligands give for the rate-controlling barriers, i.e., CO < strongly electron withdrawing phosphites < standard phosphites < aryl phosphines (and PMe_3) < higher alkyl phosphines, is in qualitative agreement with existing experimental observations of relative activities of the different classes of catalyst.[19,25,78] In addition, our calculations predict a switch in the rate-determining step, from hydrogenolysis, for the unmodified carbonyl system (due to high [substrate]/[H_2] ratios, *vide supra*) and the complexes substituted by very electron-withdrawing ligands, to the first part of the reaction (olefin coordination and insertion) for the less electron-withdrawing phosphine and phosphite systems, and this result is also in accord with observations.[18−23] In conclusion, the present investigation is the first quantum chemical study giving results in overall agreement with contemporary understanding of the mechanism and rate control in the rhodium-catalyzed hydroformylation.

Substitution also greatly affects the selectivity. β-Elimination is the key step in isomerization of higher and internal alkenes; i.e., migration of the double bond and high isomerization rates are a prerequisite to achieve one of the most important challenges in hydroformylation: selective formation of terminal linear aldehydes starting from internal alkenes.

The reaction **1** + ethylene → **5** is weakly exoergonic for the unmodified catalyst and endoergonic for the other complexes modified by phosphorus ligands. This means that, for the unmodified catalyst, the effective activation energy for the backward reaction **5** → **3** (i.e., β-elimination), in the following labeled as $\Delta G^{\ddagger}_{TS-1}$, is higher than that of the forward reaction ($\Delta G^{\ddagger}_{TS1}$ = 90 kJ/mol). The barrier to β-elimination for the unmodified catalyst is also higher than the range obtained for the phosphite-substituted catalysts ($\Delta G^{\ddagger}_{TS-1}$ = 76−82 kJ/mol). The latter catalysts thus have barriers for the backward reaction which are lower than both those of the forward reaction ($\Delta G^{\ddagger}_{TS1}$ = 85−97 kJ/mol) and the barriers to hydrogenolysis ($\Delta G^{\ddagger}_{TS4}$ = 84−91 kJ/mol); see Table 2. In contrast, triphenyl phosphine and the alkyl phosphines give rise to barriers for the backward reaction ($\Delta G^{\ddagger}_{TS-1}$ = 77−95 kJ/mol) that are lower than those of the forward reaction ($\Delta G^{\ddagger}_{TS1}$ = 104−112 kJ/mol) but higher than the barriers to hydrogenolysis ($\Delta G^{\ddagger}_{TS4}$ = 68−77 kJ/mol).

Our calculated low barriers to β-elimination for the phosphite-substituted complexes are thus commensurate with the fact that the most promising selectivities for linear aldehydes have been observed for catalysts substituted with electron-withdrawing phosphites, in general,[25] and $P(OCH_2CF_3)_3$, in particular.[79] If we narrow our focus to the elementary reaction step of β-elimination from **4** to reach the rhodium−alkene complex, **3**, that could isomerize given an alkene higher than the presently studied ethylene, $P(OCH_2CF_3)_3$ gives a catalyst with a corresponding barrier which is more than 10 kJ/mol lower than that for other phosphite−based complexes and 25 kJ/mol lower than that of any phosphine-based complex in Table 1. As noted above, electron-withdrawing ligands such as $P(OCH_2CF_3)_3$ stabilize **TS1**, and part of the lowering of the barrier to β-elimination can thus be explained by the stabilization of the transition state connecting the rhodium−ethylene complex, **3**, with the rhodium−ethyl complex, **4**. In addition, the latter complex seems to be destabilized by the presence of bulky and electron-withdrawing ligands.

Previous computational studies of rhodium-catalyzed hydroformylation have used several different model catalysts, including varying numbers of carbonyl and other donor ligands, i.e., different values of m and n in the generic formula $HRh(CO)_mL_n$ ($m + n = 4$). In addition, most studies have employed PH_3 as

(77) We have not been able to locate reports on recorded catalytic activity of PMe_3-modified rhodium catalysts for hydroformylation.

(78) Lazzaroni, R.; Settambolo, R.; Caiazzo, A. In *Rhodium Catalyzed Hydroformylation*; van Leeuwen, P. W. N. M., Clever, C., Eds.; Kluwer Academic Publishers: Dordrecht, The Netherlands, 2000.

(79) van Leeuwen, P. W. N. M.; Roobeek, K. F. *J. Organomet. Chem.* **1983**, *258*, 343.

a generic model phosphine ligand, and this complicates comparison with the present calculations. In cases where direct comparison is possible, it is generally found that our calculated relative energies for the individual elementary reaction steps are similar to those reported in other quantum chemical studies of rhodium-catalyzed hydroformylation of ethylene.[33,34] For example, using DFT (BP86), Gleich and Hutter obtained an activation free energy, $\Delta G^{\ddagger}_{298} = 51.0$ kJ/mol, for the ethylene insertion step (**3** → **4**) for L = PMe_3 only 5 kJ/mol lower than our barrier for this reaction step (Table 1). Similarly, for the elementary step of oxidative addition of H_2 (**6** → **8**), Gleich and Hutter obtained a barrier of $\Delta G^{\ddagger}_{298} = 52.2$ kJ/mol, 4 kJ/mol lower than our barrier. These moderate differences in calculated reaction energies and barriers show that the variation of computational approach, e.g., density functional, basis sets, solvent treatment, etc., does not influence the energetics to a great extent. Accordingly, the computational issues are also not the main reason for the much better agreement between theory and experiment obtained in the current study than in previous investigations. The improved agreement is partly due to the introduction of realistic ligands in the present work. Choosing correct reference states for the calculation of effective barriers, however, is even more important. For example, Decker and Cundari found CO insertion to represent the rate-determining step of hydroformylation, in disagreement with both the present results and experimental evidence.[80,81] They assumed the elementary step of ethylene insertion, **3** → **4**, to give rise to the dominating barrier in the early stages of the reaction and also left out the important CO-saturated rhodium−acyl intermediate, **7**, in the calculation of the barrier for the final part of the reaction (the hydrogenolysis). Therefore, the barriers to ethylene insertion as well as to hydrogenolysis were underestimated, and both came out (artificially) lower than the barrier to CO insertion.

3.2.2. NHC-Modified Rhodium Carbonyl Complex. In contrast to the traditional view of N-heterocyclic carbenes (NHCs) as being virtually pure σ-donors, recent quantum chemical studies have found that these ligands are also reasonably good π acceptors when bound to many transition metals.[82−84] Their bonding properties thus resemble those of phosphines,[85] although with a larger net ligand-to-metal donation.[84] The excellent donor/acceptor properties ensure that the NHC ligands typically give remarkably stable catalyst precursors with catalytic properties rivaling those of phosphine counterparts.[85] Their potential as alternatives to phosphine ligands in rhodium complexes for hydroformylation has already been explored to some extent.[86−89]

Our calculations confirm the expected similarities with respect to phosphine ligands. For example, the barriers in the first part of the reaction (ethylene coordination and insertion) are the highest calculated among the present catalysts ($\Delta G^{\ddagger}_{TS1} = 104-135$ kJ/mol)(see Table 2), and thus all three NHC ligands that are included in this study give catalysts with the coordination−insertion step being rate determining. Moreover, the least donating one of these carbenes, NHC3, gives the lowest overall calculated barrier and the most active of the presently studied NHC-based catalysts. In a recent experimental investigation of a series of Rh−NHC complexes, NHC3 was indeed found to give the most active catalyst for hydroformylation.[88]

For the ligand-modified catalysts, two different conformations have been located for the transition states of ethylene insertion, **TS1**. Characterizing these complexes in terms of a distorted trigonal bipyramid, with the hydride and a carbonyl group representing the two axial ligands, the two conformations differ in the relative positions of the modifying ligand and the equatorial carbonyl group as well as in the valence angles in the equatorial plane. In all cases, both possibilities have been tried in the calculations. Whereas the phosphine and phosphite complexes show a clear preference for the conformations shown for L = $P(OMe)_3$ and PPh_3 in Figure 3, the other conformation gives the most stable transition state for the N-heterocyclic carbene complexes, as seen for L = NHC3 in Figure 3. For the NHC ligands, these conformations are close in energy, however.[90] For example, the structure of **TS1** shown for L = NHC3 is only 4 kJ/mol more stable than the corresponding structure originating from the conformation of the phosphine and phosphite complexes. The most stable conformation for the NHC complexes features wide L−Rh−C(ethylene) angles (152°−160°) and sharp OC−Rh−C(ethylene) angles (93°−96°) in the equatorial plane.

Insertion via the most stable conformation for the carbenes leads to a square planar alkyl complex, **4**, with the two carbonyl groups positioned trans to each other.[90] The latter isomer is less stable than the structure with cis-positioned carbonyl groups shown in Scheme 1. The two sets of structures located for the carbene complexes may be interconnected through Berry pseudorotations in **TS1** and **5**.

Some characteristics of the PESs already reported above for the more electron-donating phosphines are seen to be accentuated by the NHC ligands. For this reason, the reaction profiles (Figure 2) display some features that are unique for this class of ligand: The additions of CO to **2**, **4**, and **6** are endoergonic for the carbene ligands and, for the additions to **4** and **6**, even endothermic in the case of NHC1. Thus, for the catalysts of the NHC ligands studied here, the four-coordinate hydride complex $HRh(CO)_2L$ (**2**) represents the resting state, thus contrasting all the other monosubstituted catalysts included in the present study. This result is supported by the recent observation of only two carbonyl stretching frequencies in *in situ* generated rhodium−carbonyl catalysts containing NHC3 or other N-heterocyclic carbenes.[88] The barrier to coordination−insertion is thus calculated relative to **2** for these catalysts. The fact that CO dissociation is not involved in the rate-limiting step implies that, contrary to observations for the phosphine-modified catalysts,[19] our calculations predict that CO should not have an inhibiting effect on the reaction rate.

(80) Cavalieri, d'Oro, P.; Raimondo, L.; Pagani, G.; Montrasi, G.; Gregorio, G.; Andreetta, A. *Chim. Ind. (Milan, Italy)* **1980**, *62*, 572.
(81) Gregorio, G.; Montrasi, G.; Tampieri, M.; Cavalieri, d'Oro, P.; Pagani, G.; Andreetta, A. *Chim. Ind. (Milan, Italy)* **1980**, *62*, 389.
(82) Frenking, G.; Sola, M.; Vyboishchikov, S. F. *J. Organomet. Chem.* **2005**, *690*, 6178.
(83) Jacobsen, H.; Correa, A.; Costabile, C.; Cavallo, L. *J. Organomet. Chem.* **2006**, *691*, 4350.
(84) Occhipinti, G.; Bjørsvik, H. R.; Jensen, V. R. *J. Am. Chem. Soc.* **2006**, *128*, 6952.
(85) Herrmann, W. A. *Angew. Chem., Int. Ed.* **2002**, *41*, 1290.
(86) Chen, A. C.; Ren, L.; Decken, A.; Crudden, C. M. *Organometallics* **2000**, *19*, 3459.
(87) Poyatos, M.; Uriz, P.; Mata, J. A.; Claver, C.; Fernandez, E.; Peris, E. *Organometallics* **2003**, *22*, 440.
(88) Bortenschlager, M.; Schütz, J.; von Preysing, D.; Nuyken, O.; Herrmann, W. A.; Weberskirch, R. *J. Organomet. Chem.* **2005**, *690*, 6233.
(89) Bortenschlager, M.; Mayr, M.; Nuyken, O.; Buchmeiser, M. R. *J. Mol. Catal. A: Chem.* **2005**, *233*, 67.
(90) Energies and structural data reported for the complexes of NHC ligands are in all cases those of the most stable conformers.

Similarly, the CO-saturated acyl complex (**7**) is calculated to be the undisputed lowest-lying minimum after CO insertion for the catalysts of all ligands except the NHCs and also represents the resting state for the catalysts for which hydrogenolysis is rate determining. In contrast, for the NHC ligands, the unsaturated acyl complex, **6**, is more stable than the corresponding carbonyl-saturated complex, **7**.[91] The latter complex has been observed in *in situ* IR studies of hydroformylation using the unmodified rhodium carbonyl catalysts[71−73] and phosphite−modified catalysts.[69] For the NHC-modified catalysts, our calculations suggest that if any intermediate subsequent to alkene insertion is to be observed, **6** is the most likely candidate.

The high stability of the unsaturated intermediate, **6**, is the reason for the fact that the effective barriers to hydrogenolysis for the carbene complexes do not group together with those of the electron-donating phosphines; see Table 2. The calculated activation free energies to hydrogenolysis ($\Delta G^{\ddagger}_{TS4}$) are significantly higher than those of the phosphine complexes,[91] and the strongly electron-donating NHC1 gives the highest barrier ($\Delta G^{\ddagger}_{TS4} = 113$ kJ/mol) of all those presently calculated.

3.3. Rate-Controlling Factors. We have seen that the barriers to both olefin insertion (85−135 kJ/mol) and hydrogenolysis (68−113 kJ/mol) are heavily dependent on the modifying ligand, L (Table 2). The ligands that afford low barriers in one of the reactions tend to contribute to high barriers in the other. The result is a switch in the rate-determining step from hydrogenolysis, for the unmodified carbonyl system and the complexes substituted by strongly electron-withdrawing ligands, to the first part of the reaction (olefin coordination and insertion), for the phosphine systems and moderately electron-withdrawing phosphites. We will in the following analyze in more detail the factors governing the rate of the two reactions.

3.3.1. Ethylene Coordination and Insertion. In order to separate electronic and steric effects, we initially confine our analysis to the phosphine and phosphite ligands, for which Tolman parameters are available;[92−94] see Table 3. The Tolman electronic parameter, χ, is associated with the substituents on phosphorus and is used to rank these according to the stretching frequencies of CO in (CO)Ni($PR_1R_2R_3$). Phosphorus ligands with low values for χ are considered strong σ donors, while π acceptors are associated with high values for χ. Furthermore, the assumed additivity of χ_i allows $\chi = \sum_i \chi_i$ to be defined as a property of the ligand.

The steric parameter, θ, has been defined for a symmetric ligand as the vertex angle of a cylindrical cone which has its apex located at the metal atom, 2.28 Å from the P atom, and which tangentially touches the van der Waals radii of the outermost atoms of the model.

In order to test to what extent the effective barrier to ethylene insertion ($\Delta G^{\ddagger}_{TS1}$) is controlled by steric or electronic factors, we have constructed univariate and multiple linear regression (MLR) models thereof using the Tolman parameters for the seven phosphorus ligands as independent (predictor) variables;[95] see Table 3. It turns out that $\Delta G^{\ddagger}_{TS1}$ for the monosubstituted complexes of phosphorus ligands can be predicted with good accuracy using χ alone and almost perfectly if the Tolman angle of the ligand is included as a second predictor variable. The standardized regression weights (beta weights) are $\beta_\chi = -0.87$ and $\beta_\theta = 0.19$ for the Tolman electronic parameter and cone angle, respectively. In other words, the barrier to coordination−insertion is largely governed by electronic effects. Electron-withdrawing ligands with high values for χ lower the barrier (negative correlation), whereas the opposite is true for electron-donating ligands (low values for χ). Bulky ligands, with large values for the steric parameter, θ, contribute to increase the barrier (positive correlation), albeit only moderately; see Table 4. That both increased ligand-to-metal donation and steric bulk hamper the coordination−insertion is illustrated by the fact that the calculated barrier to this reaction is significantly higher for corresponding complexes substituted by two phosphine or phosphite ligands,[96] in agreement with the lower reaction rates observed for high ligand concentrations.[18,19]

Table 4. Correlation Coefficients (R^2) of Univariate and Multiple Linear Regression Models of the Effective Reaction Barriers, $\Delta G^{\ddagger}_{TS1}$ and $\Delta G^{\ddagger}_{TS4}$[a]

predictor variables[b]	coordination–insertion	hydrogenolysis
χ alone	0.96	0.91
θ alone	0.48	0.63
χ and θ	0.98	0.99

[a] The regression models are constructed from the calculated barriers and Tolman parameters for the seven phosphorus ligands.[95] [b] Tolman electronic and steric parameters; see Table 3.

The limited influence of sterics may seem puzzling because the barriers of both olefin association[34] and insertion[33] have been postulated to be controlled mainly by steric effects, and these elementary steps constitute two-thirds of the reaction **1** → **TS1** defining our effective barrier $\Delta G^{\ddagger}_{TS1}$. However, whereas single-variable linear models of the individual reaction free energies in all cases can be established with good accuracy when based on the electronic parameter ($R^2 > 0.8$), the Tolman angle gives clearly less convincing correlations for the individual reaction steps ($R^2 < 0.5$ in all cases).

The initial dissociation step **1** → **2** is strongly facilitated by the presence of a good donor ligand, as exemplified by the N-heterocyclic carbenes. The NHC ligands basically give an ergoneutral or weakly exoergonic initial step, whereas even the most sterically demanding phosphine or phosphite ligands give a dissociation step which is endoergonic by at least 15 kJ/mol. The three carbenes included in the present study may be characterized as small compared to the bulky phosphines and phosphites. Their donor capabilities may be inspected by comparing the carbonyl stretching frequencies in the respective complexes; see Table 5. NHC1 and NHC2 are expected to be

(91) The electron-donating carbenes (NHC1, NHC2, and NHC3) give catalysts for which the unsaturated acyl complex, **6**, is calculated to be lower in energy than the corresponding carbonyl-saturated complex, **7**. For these ligands, the effective barrier to hydrogenolysis ($\Delta G^{\ddagger}_{TS4}$) is thus calculated relative to **6** instead of **7**.

(92) Tolman, C. A. *J. Am. Chem. Soc.* **1970**, *92*, 2953.

(93) Tolman, C. A. *Chem. Rev.* **1977**, *77*, 313.

(94) For the monosubstituted complexes, the mean value of the three CO stretching frequencies computed for the precursor, **1**, has been found to correlate excellently ($R^2 = 0.99$) with the χ parameter[93] of the phosphorus ligand. The χ parameter for $P(OCH_2CF_3)_3$ has therefore been predicted by using the stretching frequencies computed for $HRh(CO)_3P(OCH_2CF_3)_3$ and the linear relationship established between the frequencies in $HRh(CO)_3L$ and χ_L for L = PMe_3, PEt_3, $P(^iPr)_3$, PPh_3, $P(OMe)_3$, and $P(OPh)_3$.

(95) The correlation coefficient between θ and χ in the set of seven phosphorus ligands is low ($R^2 = 0.34$). Thus, the predictor variables are to a large extent independent, and the MLR models built thereof do not display collinearity problems.

(96) Preliminary calculations on disubstituted complexes initiating hydroformylation by CO dissociation from $HRh(CO)_2L_2$ show that, for L = $P(OMe)_3$ and PPh_3, $\Delta G^{\ddagger}_{TS1}$ is > 10 and > 20 kJ/mol higher, respectively, than the corresponding barriers quoted for the monosubstituted complexes in Table 2.

Table 5. Metal−Ligand Bond Distance (Rh−L), CO Stretching Frequencies (ν_{CO}), and Fragment Partial Charges (q) Calculated for the Catalyst Precursor, **1**[a]

L	Rh–L	ν_{CO}	$q_{Rh} + q_L$
CO	1.93	1907[b] 1911 1971	−0.05
$P(OMe)_3$	2.35	1879 1888 1937	0.13
$P(OPh)_3$	2.34	1888 1891 1938	0.07
$P(OCH_2CF_3)_3$	2.32	1901 1905 1951	0.01
PMe_3	2.40	1868 1872 1924	0.19
PEt_3	2.42	1866 1869 1922	0.20
P^iPr_3	2.47	1863 1866 1919	0.19
PPh_3	2.45	1874 1876 1927	0.14
NHC1	2.22	1845 1851 1905	0.28
NHC2	2.13	1852 1856 1911	0.27
NHC3	2.11	1865 1870 1922	0.20

[a] Charges are given in multiples of the elementary charge, frequencies, in cm^{-1}, and distances, in angstroms. $q_{Rh} + q_L$ refers to the partial charge of the combined fragment formed by the metal and the ligand. [b] Two normal modes are almost degenerate in the precursor of the unmodified catalyst, $HRh(CO)_4$.

the best σ-donors of all the present ligands, and they also give the lowest carbonyl stretching frequencies in the precursor complex, **1**. Differences in strength of the CO bonds are governed by Rh−CO π-back-donation, rather than by CO−Rh σ-donation, as can be seen from the natural population analysis (NPA)[62] charges of the Rh−L fragment in Table 5. The use of the Rh−L fragment in the population analysis avoids charge-separation problems[97] due to comparison of very different ligands. In the complexes of NHC1 and NHC2, the Rh−L fragment is more positively charged, thus confirming the increased charge donation to the carbonyl groups. Also for the rest of the ligands, the partial charge on the Rh−L fragment closely follows the trend formed by the carbonyl stretching frequencies, which also represents the expected trend in donor strength: CO < strongly electron-withdrawing phosphites < standard phosphites < aryl phosphines < alkyl phosphines < N-heterocyclic carbenes.

The reaction **1** → **3** illustrates that the present rhodium(I) complexes can be regarded as typical examples of electron-rich, low-oxidation-state organometallic compounds. This exchange reaction is endoergonic (and endothermic) in all cases and shows a clear preference for the better acceptor, the carbonyl.

Electronic effects are indeed dominating the coordination−insertion part of the hydroformylation reaction. Contributions from steric effects are smaller and to a large extent cancel between the individual elementary steps. Steric congestion facilitates dissociation of CO from **1** and makes coordination of the alkene to **2** more difficult. The overall effect of sterically bulky ligands on $\Delta G^{\ddagger}_{TS1}$ thus stems from the increased congestion in **3** and **TS1** compared to **1**, i.e., due to the trivial fact that ethylene is sterically more demanding than carbonyl. This also means that the importance of steric bulk in determining $\Delta G^{\ddagger}_{TS1}$ will increase with the size of the substrate alkene used in hydroformylation. Steric congestion has virtually no influence on the insertion step **3** → **4** and does not improve in a linear model of the corresponding change in free energy based on the electronic factor (χ) alone ($R^2 = 0.82$). The correlation between χ and the barrier to olefin insertion is negative which is consistent with the idea that a good π acceptor (high values for χ) interferes with the formation of a strong ethylene−metal bond and therefore facilitates rotation of the alkene out of the equatorial plane in order to reach the geometry of the transition state.

In transition-metal coordination catalysts for polymerization, barriers to migratory olefin insertion into metal−alkyl bonds, as measured relative to the pre-insertion metal−olefin complexes, have been found to correlate excellently with the strength of the π back-donation metal−olefin bonds in the latter complexes,[98,99] and these findings may be expected to transfer to the present reaction step involving olefin insertion into a Rh−H bond. Indeed, the C−C bond distances of ethylene in the pre-insertion complexes, **3**, are seen to increase with the donor capacities of the ligand L and, thus, also with the height of the barrier to insertion (see Figure 3). The same variation in the cost of breaking the rhodium−ethylene bond also shows up in other key bond distances; see Figure 3. The catalysts with the highest barriers to the elementary step of ethylene insertion **3** → **4** have, in accordance with Hammond's postulate,[100] transition states (**TS1**) that are located late on the reaction coordinate as judged from the lengths of the Rh−C bonds formed and the Rh−H bonds broken during ethylene insertion. The length of the forming C−H bonds does not vary much among the different optimized structures of **TS1** but show, as expected, a small decrease when going from L = CO to the more donating phosphines. The C−H distance optimized for NHC3, on the other hand, is the longest among the catalysts in Figure 3, thus suggesting that the N-heterocyclic carbenes break the trend formed by this distance as a measure for the lateness of the transition state of insertion. The discontinuity is caused by the fact that the most stable transition state for the N-heterocyclic carbene complexes is obtained for a different conformation than for the complexes of the other ligands (*vide supra*). The slightly less stable transition state originating from the same conformation as for the phosphine complexes has a shorter C−H bond distance (1.66 Å for L = NHC3) in reasonable agreement with the trend formed by the rest of the complexes. The latter conformation also features a lengthening of the Rh−L bonds in **TS1** compared to **3** which is similar to that observed for the phosphite and phosphine ligands; see Figure 3.

3.3.2. Hydrogenolysis. A linear model with the Tolman electronic parameter χ as an independent variable shows a strong correlation with the height of the barrier to hydrogenolysis ($R^2 = 0.91$); see Table 4. Including the Tolman cone angle as the second independent variable results in a close to perfect description of the barrier height by the multiple linear regression (MLR) model, showing that although the electronic properties of the ligand are dominating, both electronic and steric properties of the ligand influence the barrier. The standardized regression weights (β weights) of the MLR model are $\beta_\chi = 0.74$ and $\beta_\theta = -0.36$ for the Tolman electronic parameter and cone angle, respectively.

Whereas for the addition−insertion reaction the height of the barrier was found to correlate negatively with the electronic parameter, for hydrogenolysis it correlates positively. In other words, electron-withdrawing ligands (high values for χ) give high barriers to hydrogenolysis and low barriers to the addition−

(97) Sigfridsson, E.; Ryde, U. *J. Comput. Chem.* **1998**, *19*, 377.
(98) Jensen, V. R.; Angermund, K.; Jolly, P. W.; Børve, K. J. *Organometallics* **2000**, *19*, 403.
(99) Jensen, V. R.; Thiel, W. *Organometallics* **2001**, *20*, 4852.
(100) Hammond, G. S. *J. Am. Chem. Soc.* **1955**, *77*, 334.

insertion reaction, whereas the opposite is true for electron-donating ligands. The two reactions thus have opposite requirements to the dative ligand, which, in turn, brings about a change in the rate-determining step when moving across a set of ligands spanning a large variation in χ. The cone angle correlates negatively with the effective barrier to hydrogenolysis, meaning that a sterically demanding ligand contributes to lowering the barrier. For example, whereas trimethyl phosphine is only slightly more electron-donating than triphenyl phosphine, as judged from the electronic parameter (Table 3), the significant difference in cone angle between the two ligands shows that triphenyl phosphine clearly is the bulkier of the two. The larger steric demand of the latter ligand probably explains the slightly lower barrier to hydrogenolysis.

The direction of these correlations (*vide supra*) can be understood by considering the intermediate steps leading to the total barriers. First, the energy required in the step **7** → **8**, i.e., dissociation of CO and oxidative addition of H_2, correlates positively with the electronic factor ($R^2 = 0.92$). This is consistent with the idea that good donor ligands stabilize metal centers in higher oxidation states. Concerning the steric parameters, the Tolman angle does not show any appreciable correlation with this part of the reaction. On the other hand, the cone angle of the ligand to a large extent determines the height of the barrier for the reductive elimination **8** → **2′**.[75] The bulkier ligands facilitate elimination of the product propanal ($R^2 = 0.74$ for the linear model based on θ alone), and this is due to the higher steric pressure in the five-coordinated complex **8** than in the four-coordinated **2′**.[75]

The structure−activity relationships presented above for this reaction step suggest that the excellent donor properties of the NHC ligands should provide for facile hydrogenolysis. However, the carbenes turn out to give high effective barriers $\Delta G^{\ddagger}_{TS4}$ for this reaction, with NHC1 affording the highest calculated barrier of all the present ligands ($\Delta G^{\ddagger}_{TS4} = 113$ kJ/mol); see Table 2. This may seem surprising at first glance but is simply a result of the fact that the NHC ligand stabilizes the 16-electron acyl intermediate **6** more than the transition state to hydrogenolysis. The energy of **6** thus falls below that of the corresponding 18-electron acyl complex **7**. In other words, the barrier to hydrogenolysis for the NHC ligands has to be calculated relative to **6** instead of **7** and is not lowered to the extent predicted from the trend formed by the other ligands.[91]

3.4. Further Optimization of Monosubstituted Rhodium Carbonyl Complexes. The initial part of the hydroformylation reaction is rate determining for most of the catalysts studied in this work, indicating that this is a promising part to target if new, very active catalysts are to be developed. Moreover, the accompanying barriers ($\Delta G^{\ddagger}_{TS1}$) span a range of almost 50 kJ/mol, confirming that the catalyst performance in the coordination−insertion reaction is highly tunable. As we have seen above, there exists a clear negative correlation between the barrier height and the Tolman electronic parameter, and electron-withdrawing ligands decrease the barrier, $\Delta G^{\ddagger}_{TS1}$, with carbonyl and tris(2,2,2-trifluoroethyl) phosphite having the lowest calculated $\Delta G^{\ddagger}_{TS1}$ values. The question arises whether it would be possible to obtain even more electron-withdrawing phosphites, and to what extent such phosphites could act as activity-promoting ligands in rhodium-based hydroformylation catalysts.

In fact, the closely related tris(trifluoromethyl) phosphite has recently been calculated to have the highest semiempirical electronic parameter (SEP)[101] among all the phosphites included in a broad comparative study of stereoelectronic properties of phosphines and phosphites.[102] Although no structures involving this phosphite are currently registered in the Cambridge Structural Database, it is mentioned in the patent literature.[103,104] When subjecting the thus substituted catalyst to calculations, we do indeed confirm the expected electron-withdrawing properties of $P(OCF_3)_3$ and also show that this phosphite should lower the effective barrier to coordination−insertion by more than 10 kJ/mol compared to tris(2,2,2-trifluoroethyl) phosphite and carbonyl (see Table S2 in the Supporting Information). The pre-insertion complexes, **3**, of the two fluoroalkyl phosphines and of carbonyl are almost equally stable, and thus the remarkable lowering of the barrier calculated for the tris(trifluoromethyl) phosphite compound is exclusively caused by the elementary step of ethylene insertion, **3** → **4**. The very electron-withdrawing $P(OCF_3)_3$ prevents the formation of a strong Dewar−Chatt−Duncanson donation−back-donation bond in the pre-insertion complex and thus facilitates insertion. $P(OCF_3)_3$ gives the shortest C−C bond of ethylene in **3** and the longest forming C−H bond in **TS1** of all the presently studied P-based catalysts.

As noted above, electron-withdrawing ligands stabilize **TS1** and destabilize the rhodium−ethyl complex (**4**), thereby lowering the barrier for β-elimination. In the case of $P(OCF_3)_3$ those effects are so pronounced that the barriers **3** → **4** and **4** → **3** are equivalent. The $P(OCF_3)_3$-based catalyst is therefore predicted to show high activity in the isomerization of the double bond: a prerequisite to catalyze the formation of terminal aldehydes starting from internal alkenes.

In spite of the intense exploration of N-heterocyclic carbenes as ligands in homogeneous catalysis,[85,105] their actual use in hydroformylation[86−89] is still less developed than in, for example, palladium-catalyzed C−C coupling reactions[106−113] or ruthenium-catalyzed olefin metathesis.[115−121] One reason for the success of the NHC ligands in the latter reactions is that the transition metal center is in a higher oxidation state in the rate-limiting transition state than it is in the precursor or resting state.[84,122,123] Good donor ligands, such as N-heterocyclic carbenes, thus selectively stabilize the transition state region and thereby lower the overall barrier. In contrast, in rhodium-catalyzed hydroformylation, two different parts of the reaction may be rate determining, coordination−insertion and hydrogenolysis (see Figure 1), and these involve the rhodium metal

(101) Gillespie, A. M.; Pittard, K. A.; Cundari, T. R.; White, D. P. *Internet Electron. J. Mol. Des.* **2002**, *1*, 242.
(102) Cooney, K. D.; Cundari, T. R.; Hoffman, N. W.; Pittard, K. A.; Temple, M. D.; Zhao, Y. *J. Am. Chem. Soc.* **2003**, *125*, 4318.
(103) Yoshimura, S.; Nakajima, H.; Kamino, M. Jpn. Kokai Tokkyo Koho, JP 2002231309, 2002.
(104) Okamoto, T.; Yoshimura, S.; Fujitani, N. Jpn. Kokai Tokkyo Koho, JP 2002025609, 2002.
(105) Peris, E.; Crabtree, R. H. *Coord. Chem. Rev.* **2004**, *248*, 2239.
(106) Moncada, A. I.; Manne, S.; Tanski, J. M.; Slaughter, L. M. *Organometallics* **2006**, *25*, 491.
(107) Clement, N. D.; Cavell, K. J.; Ooi, L. L. *Organometallics* **2006**, *25*, 4155.
(108) Marion, N.; Navarro, O.; Mei, J. G.; Stevens, E. D.; Scott, N. M.; Nolan, S. P. *J. Am. Chem. Soc.* **2006**, *128*, 4101.
(109) Viciu, M. S.; Germaneau, R. F.; Nolan, S. P. *Org. Lett.* **2002**, *4*, 4053.
(110) Kremzow, D.; Seidel, G.; Lehmann, C. W.; Fürstner, A. *Chem.−Eur. J.* **2005**, *11*, 1833.
(111) Christmann, U.; Vilar, R. *Angew. Chem., Int. Ed.* **2005**, *44*, 366.
(112) Viciu, M. S.; Kissling, R. M.; Stevens, E. D.; Nolan, S. P. *Org. Lett.* **2002**, *4*, 2229.
(113) McGuinness, D. S.; Cavell, K. J.; Skelton, B. W.; White, A. H. *Organometallics* **1999**, *18*, 1596.

Table 6. Effective Free Energies and Enthalpies (in Parentheses) of Activation Calculated for the Suggested New Catalysts $HRh(CO)_3L$[a]

L	$\Delta G^{\ddagger}_{TS1}$	$\Delta G^{\ddagger}_{TS2}$	$\Delta G^{\ddagger}_{TS4}$
$P(OCF_3)_3$	72 (69)	49 (48)	94 (99)
NHC4	98[b] (55)[b]	79[c] (37)[c]	84[d] (59)[d]
NHC5	103[b] (59)[b]	62[c] (28)[c]	78[d] (51)[d]

[a] All energies are given in kJ/mol. [b] The barrier is calculated relative to **2** (for the relative free energies, see Table S2). [c] The barrier is calculated relative to **4** (for the relative free energies, see Table S2). [d] The barrier is calculated relative to **6** (for the relative free energies, see Table S2).

Chart 2. Dative Ligands Predicted To Provide New, Highly Active Catalysts, $HRh(CO)_3L$, for the Hydroformylation Reaction; See Table 6

$P(OCF_3)_3$

NHC 4

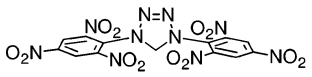

NHC 5

center in two different oxidation states. Therefore, it is not obvious that maximizing donation of electron density to the metal center in a hydroformylation catalyst will result in very high catalytic activity. In fact, as already pointed out (*vide supra*), for most of the catalysts, the coordination−insertion part seems to be rate-limiting. And, in this early stage of the reaction, the metal center is in oxidation state I, just as in the catalyst precursor. Coordination−insertion is rate determining for all three NHC-based catalysts reported in Table 2, and we predict the least donating NHC ligand (NHC3) to give the most active of the Rh−NHC complexes. The task of further improvement of catalytic activity for NHC-based catalysts for hydroformylation should therefore be one of reducing the donating capacity, or increasing the π-acceptor capacity, of the carbene ligand. The N-heterocyclic carbenes are usually thought of as excellent and virtually pure σ donors. The quest for activity-promoting NHC ligands in rhodium-catalyzed hydroformylation thus also implies answering the general and fundamental question of how tunable the electronic properties of these carbenes are and to what extent their π-acidity may be increased.

To address these questions, we have included two novel N-heterocyclic carbenes in our survey; see Chart 2 and Table 6 as well as Tables S2 and S3 in the Supporting Information. These two carbenes incorporate strongly electron-withdrawing substituents, CF_3 in NHC4 and 2,4,6-trinitro phenyl in NHC5, at the nitrogen atoms of the amine groups in the carbene ring.[124] In other words, these carbenes may be thought of as modifications of the tetrazol-based carbene, NHC3, which actually has been observed to perform well as a ligand in hydroformylation.[88] The two suggested substituents are of very different size and thus also ensure that the effect of different steric requirements are probed in the calculations. The effect of introducing these substituents is one of reducing the barrier to both coordination−insertion, by 6 kJ/mol (NHC4) and 1 kJ/mol (NHC5), and hydrogenolysis, by 5 kJ/mol and 10 kJ/mol (NHC5), compared to the Rh−NHC3 catalyst (see Table 2). For NHC4, the barrier to coordination−insertion thus is below 100 kJ/mol and is comparable to the corresponding barriers obtained for the phosphite- rather than the phosphine-modified catalysts. This can be understood by comparison of the calculated carbonyl stretching frequencies and partial charges; see Tables 5 and S4 in the Supporting Information. Whereas the electron-donating/accepting properties of NHC3 are similar to those of alkyl phosphines, the new carbenes, NHC4 and NHC5, group together with the phosphites in this respect. In other words, substitution brings about a pronounced change in the electronic properties of the carbene.

The lowering of the barrier to hydrogenolysis comes as a result of reduced stability for the unsaturated intermediate, **6**, and, in the case of NHC5, also increased steric requirements which are known to reduce this barrier (*vide supra*). The rate-determining step remains one of coordination−insertion as in the case for the other NHC-based catalysts. The new catalysts based on NHC4 and NHC5 are predicted to have activities which are similar to or higher than that of NHC3. NHC4 and NHC5 are seen to have comparable electronic properties, as judged from the carbonyl stretching frequencies and fragment charges in Table S4 in the Supporting Information.

The lower catalytic activity predicted for NHC5 can thus to a large extent be attributed to steric bulk. This leads us to the general conclusion that significant improvement in activity of NHC-based rhodium catalysts for hydroformylation may be obtained by continued ligand optimization aimed at increasing the electron-withdrawing capacity of the carbene through substitution at the amine nitrogen atoms in tetrazol-based carbenes. The steric requirements of the new ligands, however, should not be increased much beyond that of the parent tetrazol design, NHC3.

4. Conclusions

We have performed a molecular-level computational investigation of the hydroformylation of ethylene for a range of monosubstituted rhodium−carbonyl catalysts, $HRh(CO)_3L$. The reaction can be partitioned into three main sections: coordination−insertion of ethylene, coordination−insertion of CO, and hydrogenolysis. Analysis of our computed potential energy surfaces allows us to identify effective barriers, consisting of

(114) McGuinness, D. S.; Cavell, K. J. *Organometallics* **2000**, *19*, 741.
(115) Grubbs, R. H. *Angew. Chem., Int. Ed.* **2006**, *45*, 3760.
(116) Astruc, D. *New J. Chem.* **2005**, *29*, 42.
(117) Scholl, M.; Ding, S.; Lee, C. W.; Grubbs, R. H. *Org. Lett.* **1999**, *1*, 953.
(118) Huang, J. K.; Stevens, E. D.; Nolan, S. P.; Petersen, J. L. *J. Am. Chem. Soc.* **1999**, *121*, 2674.
(119) Frenzel, U.; Weskamp, T.; Kohl, F. J.; Schattenman, W. C.; Nuyken, O.; Herrmann, W. A. *J. Organomet. Chem.* **1999**, *586*, 263.
(120) Ackermann, L.; Fürstner, A.; Weskamp, T.; Kohl, F. J.; Herrmann, W. A. *Tetrahedron Lett.* **1999**, *40*, 4787.
(121) Scholl, M.; Trnka, T. M.; Morgan, J. P.; Grubbs, R. H. *Tetrahedron Lett.* **1999**, *40*, 2247.
(122) Braga, A. A. C.; Ujaque, G.; Maseras, F. *Organometallics* **2006**, *25*, 3647.
(123) Goossen, L. J.; Koley, D.; Hermann, H. L.; Thiel, W. *J. Am. Chem. Soc.* **2005**, *127*, 11102.
(124) Imidazol-based NHC ligands with electron-withdrawing substituents at the nitrogen atoms have been achieved.[125] Metal complexes of tetrazol-based carbenes are difficult to synthesize since the intermediate tetrazolinylidene decomposes in the presence of a base.[126,127] However, electron-withdrawing substituents should increase rather than decrease the stability of the tetrazolinylidene and thus facilitate synthesis of metal complexes coordinated by such tetrazol-based carbenes.
(125) Ritter, T.; Day, M. W.; Grubbs, R. H. *J. Am. Chem. Soc.* **2006**, *128*, 11768.
(126) Herrmann, W. A.; Schütz, J.; Frey, G. D.; Herdtweck, E. *Organometallics* **2006**, *25*, 2437.
(127) Zimmermann, W.; Olofson, R. A. *Tetrahedron Lett.* **1970**, 3453.

combined elementary reaction steps, for these three stages of the hydroformylation reaction. For the unmodified catalyst and for catalysts modified by electron-withdrawing phosphites, an 18-electron acyl rhodium complex has been identified as the resting state, and the rate-determining reaction is found to be that of hydrogenolysis, in agreement with experiment.[71−73] For the catalysts modified by more electron-donating ligands, the rate-determining reaction is found to be that of coordination−insertion of ethylene, and our calculations thus predict a switch in the rate-controlling step, between hydrogenolysis and coordination−insertion of ethylene, when moving across a spectrum of modifying ligands with varying electronic properties. This property of rhodium-catalyzed hydroformylation has been observed in kinetic investigations.[69] Finally, the calculated ordering of ligands with increasing rate-controlling barriers, CO < strongly electron-withdrawing phosphites < standard phosphites < aryl phosphines (and PMe_3) < higher alkyl phosphines, is in qualitative agreement with existing experimental observations of relative activities of the different classes of catalyst. The improved agreement with experiment compared to previous computational investigations can to a large extent be attributed to the fact that the present reaction barriers consistently are calculated relative to the most stable minima at the entrance of each section of the hydroformylation reaction. For the phosphine- and phosphite-modified catalysts, this means that the barriers to coordination−insertion and hydrogenolysis are calculated relative to 18-electron hydride and acyl resting states, respectively. For the N-heterocyclic carbenes, these barriers are calculated relative to the corresponding 16-electron hydride and acyl complexes which turn out to be more stable in the presence of such excellent donor ligands.

Sound theoretical treatment should represent a potent tool for further development and optimization of ligands and catalysts. We have investigated this potential by also subjecting to calculation complexes that have yet to be reported experimentally. Calculations on the $P(OCF_3)_3$-modified catalyst show that the barrier to coordination−insertion may be lowered drastically by increasing the electron-withdrawing capacity of phosphite ligands compared to contemporary electron-withdrawing phosphites. The resulting catalysts are furthermore predicted to have very low barriers to β-elimination from the rhodium−alkyl intermediates and are thus expected to show improved activity for the formation of linear aldehydes starting from internal alkenes. We have also included two novel tetrazol-based NHC ligands in our survey. We have shown that it is possible to increase the electron-withdrawing capacity of these carbenes even further through directed substitution at the amine nitrogen atoms. Substitution brings the electron-donating/accepting properties of the carbenes into the realm of the phosphites, which also translates into lower effective reaction barriers, to approach those of the phosphites. In conclusion, our predictions show that significant improvement in activity of existing phosphite- or carbene-based rhodium catalysts for hydroformylation may be obtained by increasing the electron-withdrawing capacity of the modifying ligand.

Acknowledgment. The Norwegian Research Council is gratefully acknowledged for financial support through the NANOMAT program (Grant No. 158538/431) and the Strategic University Program in Quantum Chemistry (Grant No. 154011/420) as well as for grants of computer time through the Norwegian High Performance Computing Consortium (NOTUR).

Supporting Information Available: Complete Computational Details section including full ref 52 (given as ref 1, page S5), relative enthalpies, free energies and properties for the three predicted, new catalysts, energies and Cartesian coordinates of all optimized structures, and effective core potentials (ECPs) and basis sets used in the calculations (PDF). This material is available free of charge via the Internet at http://pubs.acs.org.

JA070395N